JOURNAL OF Applied Polymer SCIENCE

"One-Pot" Synthesis of Well-Defined Functional Copolymer and Its Application as Tumor-Targeting Nanocarrier in Drug Delivery

Chenhong Wang,[1] Lei Qiao,[1] Husheng Yan,[2] Keliang Liu[1]

[1]Beijing Institute of Pharmacology and Toxicology, Beijing 100850, China

[2]Key Laboratory of Functional Polymer Materials (Ministry of Education) and Institute of Polymer Chemistry, Nankai University, and Collaborative Innovation Center of Chemical Science and Engineering (Tianjin), Tianjin 300071, China

Correspondence to: H. Yan (E-mail: yanhs@nankai.edu.cn); K. Liu (E-mail: keliangliu55@126.com)

ABSTRACT: A one-pot synthesis is developed for PEG_{600}-*b*-poly(glycerol monoacrylate) (PEG_{600}-*b*-PGA), by which folate and superparamagnetic iron oxide nanoparticles (SPIONs) are assembled to form folic acid-conjugated magnetic nanoparticles (FA-MNPs) as a tumor targeting system. The synthesis consists of a "click" reaction and atom transfer radical polymerization (ATRP) to obtain the well-defined furan-protected maleimido-terminated PEG_{600}-*b*-poly(solketal acrylate) (PEG_{600}-*b*-PSA) copolymer. After deprotection, the key copolymer *N*-maleimido-terminated PEG_{600}-*b*-PGA is successfully conjugated with thiol derivatives of folate and FITC, respectively. FA-MNPs are developed by assembling of the resulting polymer FA-PEG_{600}-*b*-PGA with SPIONs, and characterized for their size, surface charge, and superparamagnetic properties. To investigate the cellular uptake of the nanoparticles by Hela cells and φ2 cells using fluoresce technique, FA-FITC-MNPs are also obtained by assembling of FA-PEG_{600}-*b*-PGA, FITC-PEG_{600}-*b*-PGA with SPIONs. Qualitative and quantitative determinations of FA-FITC-MNPs show that the particles specifically internalized to Hela cells. No significant cytotoxicity is observed for these two kinds of cell lines. © 2014 Wiley Periodicals, Inc. J. Appl. Polym. Sci. **2014**, *131*, 40405.

KEYWORDS: drug delivery systems; magnetism and magnetic properties; nanoparticles; nanowires and nanocrystals; radical polymerization

Received 17 October 2013; accepted 5 January 2014

DOI: 10.1002/app.40405

INTRODUCTION

Superparamagnetic iron oxide nanoparticles (SPIONs) with diameters less than 20 nm are favored for biomedical applications because of their biocompatibility, easy preparation, and superparamagnetic behavior, which prevent undesired magnetic agglomeration without an external magnetic field.[1] Therefore, SPIONs have been developed not only as an excellent contrast-enhancing agent in magnetic resonance imaging (MRI)[2,3] but also as carriers in targeted drug delivery systems that are directed to the desired sites by external magnetic fields.[4,5] More importantly, this targeting property is further enhanced by targeting ligands, such as monoclonal antibodies,[6] peptides,[7] and small molecules,[8,9] for improving cellular and nuclear uptake. Folic acid (FA) is well known to have a high affinity to the cell surface folate receptor (FR), which is overexpressed by several human tumors, including cancer of the ovaries, kidney, colon, lung, colon, and breast, and is restricted in normal tissues.[10–12] Many reports have described that SPIONs conjugated to folate exhibit active targeting to tumor cells.[13–15]

We have developed a new kind of SPION coated with polyethylene glycol-*b*-poly(glycerol monoacrylate) (PEG-*b*-PGA), with a size of approximately 50–70 nm, which can be stably dispersed in water for more than 1 year.[16] Folate-tetra(ethylene glycol)-poly(glycerol monoacrylate) (FA-TEG-PGA) was further synthesized in which only 70% NH_2-TEG-PGA was attached to FA by amide bonds; then, FA-TEG-PGA-coated magnetic nanoparticles that targeted cancer cells were prepared.[17] However, the cell uptake ability of these magnetic nanoparticles decreased with an increase of FA content, which might be related to the structure of FA-TEG-PGA. Although the PGA segment provided the multidentate interactions with iron atoms at the SPION surface, tetra(ethylene glycol) (M_w:194) might be too short to enhance the solubility of the FA (M_w: 441) segment.

In this article, we report on the design and synthesis of the novel well-defined functional copolymer *N*-maleimido-terminated-PEG_{600}-*b*-PGA. This copolymer was synthesized via the combination of a "click" reaction and atom transfer radical polymerization (ATRP) in a one-pot process. "Click reactions," as termed by Sharpless and coworkers,[18] have gained great attention because of their high specificity, quantitative yields, and nearly perfect fidelity in the presence of multiple functional groups.[19,20] ATRP[21–23] is a particularly attractive controlled

Additional Supporting Information may be found in the online version of this article.

radical polymerization process for the synthesis of polymers with a predetermined degree of polymerization and narrow molecular weight distribution (low polydispersity, M_w/M_n).[24] The combination of these two techniques in a one-pot synthesis has been investigated because ATRP not only shares a number of attractive features with "click" reactions, such as a high tolerance toward a wide range of functional groups and protic solvents, but it also uses the same copper catalyst system.[25–28] Herein, the combination of ATRP and "click" chemistry provides three advantages. First, by using the "click" reaction, a polymer with a highly reactive maleimido-terminal group is synthesized that can further efficiently conjugate to thiol derivatives. Second, ATRP allows the construction of polymer chains to conjugate to the nanoparticle surface, and its controlled polymerization characteristics offer the same complexation ability. Third, the combination simplifies the synthesis and achieves the polymer with high purity. Thus, the well-defined *N*-maleimido-terminated-PEG$_{600}$-*b*-PGA with high purity was achieved by one-pot process. Then, FA-PEG$_{600}$-*b*-PGA or FITC-PEG$_{600}$-*b*-PGA was respectively synthesized by conjugating thiol derivates of FA or FITC. Finally, FA-conjugated magnetic nanoparticles (FA-MNPs) were obtained by self-assembly of FA-PEG$_{600}$-*b*-PGA with SPIONs, and FA-FITC-conjugated magnetic nanoparticles (FA-FITC-MNPs) were prepared by FA-PEG$_{600}$-*b*-PGA, FITC-PEG$_{600}$-*b*-PGA with SPIONs. These magnetic nanoparticles have shown highly efficient, specific tumor targeting and lower cytotoxicity *in vitro* experiments.

EXPERIMENTAL

Materials

2-Bromoisobutyryl bromide (98%), *N*, *N*, *N*′, *N*″, *N*‴-pentamethyldiethylenetriamine (PMDETA, 99+%), 1,3-dicyclohexylcarbodiimide (DCC), hydroxybenzotriazole (HOBt), trifluoroacetic acid (TFA), thioanisole, ethanedithiol, and anisole were purchased from Sigma-Aldrich and were used without further purification. Fmoc-Cys(Trt) and Boc-Lys(Fmoc) were from Chengnuo Ind (China). Rink amide MBHA resin (0.8 mmol/g) was from Nankai Hecheng (China). Copper (I) bromide (CuBr) was purified by washing with glacial acetic acid, followed by absolute ethanol and acetone, and then dried under vacuum. PEG$_{600}$ was dried with toluene by azeotropic distillation before use. Solketal acrylate (SA) was prepared according to the procedure previously described[29] and stored at 4°C under argon atmosphere. ^{1}H NMR (400 MHz, $CDCl_3$, δ): 6.43–5.88 (m, 3H, CH_2=C*H*), 4.50–3.70 (m, 5H, CH_2CHCH_2), 1.44, 1.38 (s, 6H, $C(CH_3)_2$). All other solvents were redistilled from drying reagents, respectively. FA (≥97%) was purchased from Sigma-Aldrich (St. Louis, MO) and used as received.

Preparation of Magnetic Nanoparticles

One-Pot Synthesis of N-maleimido-Terminated PEG$_{600}$-b-PGA via a Click Reaction and ATRP. CuBr (0.013 g, 0.090 mmol), PMDETA (0.039 g, 0.246 mmol), compound **1** (0.80 g, 1.0 mmol, See Supporting Information), compound **2** (0.35 g, 1.0 mmol, See Supporting Information), SA (3.0 mL, 20.0 mmol), and cyclohexanone (4.0 mL) were added to a Schlenk flask. After stirring for 4 h at room temperature, the temperature was increased to 80°C to promote SA polymerization. To monitor the reaction, samples were withdrawn periodically for gel permeation chromatography (GPC) analysis. After 6 h, the reaction was stopped by exposure to air and diluted with acetone. The solution was filtered through a column filled with neutral alumina to remove the copper complex, and the polymer was precipitated in cold hexane. The resulting polymer furan-protected maleimido-terminated PEG$_{600}$-*b*-poly(solketal acrylate) (PEG$_{600}$-*b*-PSA) (3.6 g) was dissolved in toluene (30 mL) and refluxed at 120°C for 7 h. After cooling the mixture to ambient temperature, the solvent was evaporated under reduced pressure and then precipitated into cooled petroleum ether. A solution of *N*-maleimido-terminated PEG$_{600}$-*b*-PSA (3.2 g) in acetone (20 mL) was cooled to 0°C, to which HCl (1*N*, 9.0 mL) was added dropwise. The resulting turbid solution was stirred at room temperature for 24 h. The solution became clear after water (20 mL) was added. The resulting solution was dialyzed (MWCO 3500) against water until the pH was neutral and subsequently lyophilized to obtain *N*-maleimido-terminated PEG$_{600}$-*b*-PGA (2.5 g) as a white solid. ^{1}H NMR (400.03 MHz, D_2O, 298 K, δ): 6.69 (s, CH_{vinyl}), 4.24, 4.10, 3.75 (OCH_2C*H*OCH_2O), 3.70–3.60 (CH_2CH_2O), 2.33, 1.90, 1.68 (CH_2C*H*).

Preparation of the FA-PEG$_{600}$-b-PGA Copolymer

The copolymer FA-PEG$_{600}$-*b*-PGA was synthesized according to previous work.[30] In brief, the peptide was synthesized by standard solid phase peptide synthesis (SPPS) using Fmoc protocols with DCC and HOBt as the coupling reagents. Fmoc-Cys(Trt) and Boc-Lys(Fmoc) were anchored to Rink amide MBHA resin (0.8 mmol/g, 0.125 g) in succession. After removal of the Fmoc group from the side-chain amino group of Lys, it was treated with 0.4 mmol of FA in 5 mL of DMSO overnight. The reaction was verified by a negative ninhydrin reaction. Then, the peptide was cleaved using 10 mL of TFA/thioanisole/ethanedithiol/anisole (90/5/3/2) for 3 h at room temperature and precipitated by adding cold ether (−20°C). The precipitate was filtered and washed with 3 × 20 mL portions of cold ether, and the peptide was dissolved in deionized water and lyophilized. Crude peptides were purified using C18 reversed-phase high-performance liquid chromatography (RP-HPLC) and analyzed by matrix-assisted laser desorption/ionization-time of flight mass spectrometry (MALDI-TOF). The mass of the peptide Lys(FA)-Cys-NH_2 was measured to be 571.6 (calculated as 571).

A 2.0 × 10^{-5} mol sample of *N*-maleimido-terminated PEG$_{600}$-*b*-PGA (M_n: 5.5 × 10^3 by GPC) and 4.0 × 10^{-5} mol of Lys(FA)-Cys-NH_2 were dissolved in 5 mL of deionized water. The mixture was stirred at room temperature, and the reaction was monitored by HPLC. After the reaction was complete, the unreacted peptide was removed by placing the mixture in dialysis tubing (MWCO 3500) and dialyzing the reaction mixture four times against water over 48 h (Spectra/Por, Laguna Hills, CA). The yellow polymer FA-PEG$_{600}$-*b*-PGA was obtained after freeze drying. The ^{1}H NMR peak at 6.69 ppm, assigned to the double bonds of the maleimido group, disappeared after the reaction. The polymer FITC-(*ω*-Ahex)-Cys-PEG$_{600}$-*b*-PGA was also synthesized using the above method.

Preparation of FA-MNP, FA-FITC-MNP, and mPEG-MNP

$HClO_4$-stabilized Fe_3O_4 magnetic nanoparticles were prepared according to our previously described method.[17] The final

particle concentration was 32 mg/mL, which was determined by evaporating approximately 2 mL of the colloid to dryness.

A 100 mg sample of the block polymer (FA-PEG_{600}-*b*-PGA, the mixture of FITC-(ω-Ahex)-Cys-PEG_{600}-*b*-PGA and FA-PEG_{600}-*b*-PGA, or $mPEG_{2000}$-*b*-PGA) was dissolved in 5 mL of deionized water, and 200 μL of $HClO_4$-stabilized Fe_3O_4 magnetic nanoparticles was added. The mixture was stirred under argon for 24 h and then centrifuged (15,000*g* relative centrifugal forces, 20 min) to sediment the nanoparticles. After removing the supernatant, the sediment could be easily dispersed in deionized water by shaking or sonication. The sedimentation and dispersion cycle was repeated three times to remove any remaining polymer. The final nanoparticles were dispersed in deionized water.

Characterization

^{1}H-NMR spectra were recorded on a JNM-ECA-400 spectrometer operating at 400 MHz with tetramethylsilane as the internal standard at room temperature. GPC was performed using a Waters 515 HPLC pump, a Waters 2414 refractive index detector, and three Styragel columns (HT-2, HT-3, and HT-4). Linear polystyrene standards were used as calibration samples. The eluent was anhydrous tetrahydrofuran, and the flow rate was 1.0 mL/min. Peptides and conjugates were analyzed using RP-HPLC with a linear gradient and a flow rate of 1.0 mL/min, in a mobile phase consisting of (A) 0.1% aqueous TFA and (B) 0.1% TFA in 70% aqueous acetonitrile (ACN). The fractions were analyzed using a Shimadzu LC-10AT VP Plus liquid chromatograph with an SPD-10A VP Plus UV-Vis detector operating at 210 nm and equipped with a WondaSil™ (C18 column, 5 μm, 4.6 × 150 mm GL Sciences, Japan) reverse-phase column. MALDI-TOF mass spectra were recorded on a Bruker Reflex mass spectrometer (Bruker Daltonics, USA) by positive electrospray mode using α-cyano-4-hydroxycinnamic acid as the matrix and a mixture of TFA/ACN/H_2O as the solvent. The UV-Vis absorbance was measured using a UV-2550 detector (Shimadzu, Japan). The hydrodynamic size and surface charge of the nanoparticles were determined using a Zetasizer NanoZS90 instrument (Malvern Instrument, Worcestershire, UK) fitted with a 633-nm laser at a fixed scattering angle of 90°. The magnetic nanoparticles were dispersed in deionized water from a Milli-Q® ultra-pure water system, and the concentration was approximately 1 mg/mL. Each measurement was repeated at least five times, and the results were reported as average ± standard deviation. The magnetization of the magnetic nanoparticles was measured as a function of the applied magnetic field H with a 7410 VSM (Lakeshore, USA) superconducting quantum interference device (SQUID) magnetometer. The hysteresis of the magnetization was obtained by changing H between +20k and −20kOe at 300 K.

In Vitro Evaluation Experiments

Cell Culture. Human cervical carcinoma Hela cells and mouse fibroblast φ2 cells were purchased from the Cell Resource Center of Peking Union Medical College (Beijing, China) and cultured with regular growth medium consisting of RPMI 1640 medium (Gibco, USA) supplemented with 10% fetal bovine serum (FBS; Gibco) and 5% penicillin–streptomycin in a humidified atmosphere with 5% CO_2 at 37°C.

In Vitro Evaluation of Folate Receptor Targeting Using Flow Cytometry

To investigate the cellular uptake behavior of FITC-FA-MNP by different cell lines, Hela cells and φ2 cells were, respectively, seeded in 12-well plates at a density of 2.5×10^5 cells per well and incubated for 24 h. Then, 0.2 mg/mL FITC-FA-MNPs in folate-deficient RPMI-1640 medium (Gibco) was added to each of the wells, and the cells were incubated for 2, 4, or 24 h. After incubation, the cells were harvested with 0.25% (w/v) trypsin–0.02% (w/v) EDTA solution, transferred to fluorescence activated cell sorting (FACS) tubes (Becton Dickinson), and spun down. Cells were analyzed on a FACSCalibur flow cytometer (Becton Dickinson, Franklin Lakes, NJ). The excitation wavelength was 488 nm, and the fluorescence was measured with the FL1 channel. A total of 10,000 cells per sample were analyzed. The number of cells with fluorescence intensity greater than that of unlabeled cells was used to determine the fraction of labeled cells. The baseline was obtained by analyzing unlabeled control cells. The relative median fluorescence (RMF) was calculated by dividing the median of the labeled cells by the median of an unlabeled cell population.

In Vitro Evaluation of Folate Receptor Targeting Using Live-Cell Imaging

To determine the location of FA-FITC-MNPs in the different cell lines, Hela cells and φ2 cells were, respectively, seeded at a concentration of 5×10^4 cells/mL in 35 mm glass bottom culture dishes (Mat-Tek Corporation, Ashland, MA) with glass cover slips and grown for 24 h. The cells were incubated with wheat germ agglutinin (WGA), Alexa Fluor® 594 conjugate (5 μg/mL, Invitrogen, Eugene, OR) for 5 min. After washing three times with phosphate-buffered saline (PBS), the cells were incubated in PBS containing 0.5 mg/mL FA-FITC-MNPs for 60 min and washed three times with PBS. The Hela cells and φ2 cells were kept in PBS throughout imaging. Cells were observed with an inverted microscope (PerkinElmer UltraVIEW VoX, PerkinElmer, UK) spinning disk confocal microscope equipped with cover slip chambers at 37°C and CO_2 (5%) control. For image acquisition, a 60× oil immersion objective (1.3NA) was used with a Hamamatsu Orca AG CCD camera. The microscope was equipped with two separate diode-pumped solid state laser lines (488 and 561 nm). For fluorescence imaging of FA-FITC-MNPs, an excitation wavelength (λ_{ex}) of 488 nm was used exclusively. The time-lapse images were collected at room temperature at 120-ms time intervals over 1 s. The two movies in the Supporting Information were edited using Volocity acquisition software.

FITC-MNP Uptake by Hela Cells and φ2 Cells Using Confocal Microscopy

Hela cells and φ2 cells were, respectively, seeded at a concentration of 5×10^4 cells/mL in 35 mm glass bottom culture dishes (Mat-Tek Corporation, Ashland, MA) with glass cover slips and grown for 24 h. Both two cells were incubated for 2 h in complete media containing FITC-MNP (0.5 mg/mL) and washed three times with PBS. The cells were fixed in PBS – 4% formaldehyde for 10 min at room temperature. After washing three times with PBS, the cells were examined using a Carl Zeiss LSM 510 meta fluorescence microscope with long focal length optics and excitation using green He-Ne (543 nm) lasers.

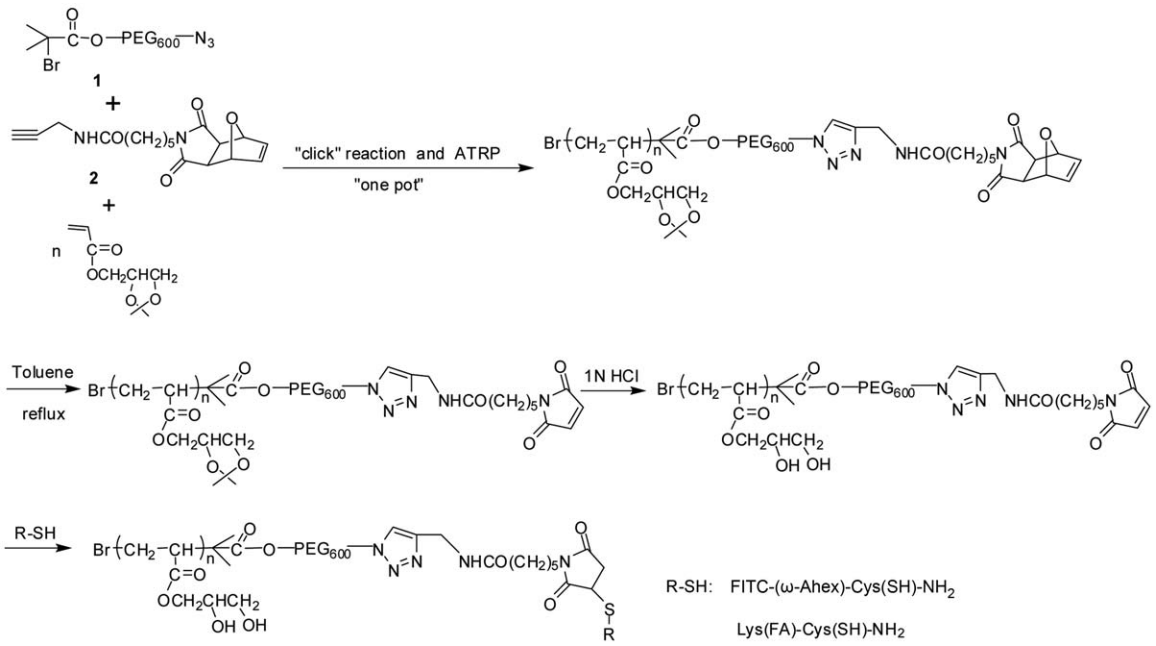

Scheme 1. Schematic representation of the synthesis of FA-PEG$_{600}$-*b*-PGA and FITC-PEG$_{600}$-*b*-PGA.

In Vitro Evaluation of Folate Receptor Targeting Using Transmission Electron Microscopy

To compare the uptake ability of FA-MNPs and mPEG-MNPs, Hela cells were plated in T-25 flasks at a concentration of 5.0×10^5 cells per well and incubated for 24 h. Then, 0.2 mg/mL FA-MNPs or mPEG-MNPs in folate-deficient RPMI-1640 medium were, respectively, added to the cells and incubated for 24 h. The cells were washed twice with PBS, harvested with 0.25% (w/v) trypsin–0.02% (w/v) EDTA solution, centrifuged, and resuspended in 5 mL of Karnovsky's fixative for 24 h. After fixation, the cells were processed in agar and embedded in epoxy for sectioning. Cell sections were stained with osmium tetroxide, lead citrate, and uranyl acetate for TEM-contrast enhancement. Cell images were taken using a Hitachi H-7650 TEM microscope operated at 80 kV.

Cytotoxicity Assay Using the MTS Assay

Hela cells and φ2 cells were, respectively, seeded in 96-well cell culture plates (Corning, Corning, NY) at a density of approximately 1×10^4 cells per well in RPMI-1640 supplemented with 10% (v/v) fetal calf serum and incubated for 24 h. The cells were washed twice with PBS and incubated with 100 μL of FA-MNPs suspended in folate-deficient RPMI-1640 medium at the indicated concentration at 37°C for 24 h. The cells were washed with PBS to remove the nanoparticles and suspended in 80 μL of PBS. Thereafter, 20 μL of Cell Titer 96® AQ_{ueous} One Solution Reagent (Promega Corp., Madison, WI) was added to each well, followed by an incubation period of 2 h. The solution absorbance was measured at 490 nm using a SpectraMax® M5 spectrophotometer (Molecular Devices). PBS was used as a negative control. Cell viability data were obtained by calculating the ratio of viable cells in the treated cultures to the untreated control cells. The experiment was repeated five times for each nanoparticle concentration.

RESULTS AND DISCUSSION

Synthesis of FA-PEG$_{600}$-*b*-PGA and FITC-PEG$_{600}$-*b*-PGA

Reactions with high yield, moderate reaction conditions, and high specificity, such as "click" reactions and thiol reactions with maleimido groups, are widely used in polymer chemistry.[31,32] To obtain a well-defined functional polymer, we designed and synthesized *N*-maleimido-terminated-PEG$_{600}$-*b*-PGA, which can couple thiol derivatives with high efficiency. The copolymer was synthesized by ATRP; however, maleimido derivatives could participate in free radical polymerization[33,34] to get random copolymers. Therefore, the reversible Diels-Alder reaction was chosen to protect the maleimido group before polymerization. Accordingly, the copolymer furan-protected maleimido-PEG$_{600}$-*b*-PSA was synthesized via the combination of a "click" reaction and ATRP in "one pot". Then, the resulting polymer *N*-maleimido-terminated-PEG$_{600}$-*b*-PGA was achieved after deprotection of furan and the ketal group (Scheme 1).

Interestingly, the catalyst Cu (I) can be used simultaneously in "click" reactions and ATRP. The copolymer furan-protected maleimido-terminated PEG$_{600}$-*b*-PSA was obtained via a combination of a "click" reaction and ATRP in a "one-pot" process. After compound ***1***, compound ***2***, and SA were mixed in a flask according to the designed ratio simultaneously, the "click" reaction was performed at room temperature in the presence of CuBr/PMDETA. The ^{1}H NMR analysis revealed that the quantitative conversion of the azide group was achieved within 4 h. The polymerization of SA was conducted at 80°C. GPC showed that the molecular weight of the resulting polymer was linearly correlated with the polymerization time, and the polydispersity index (PDI) was kept between 1.16–1.21 (Figure 1). The reaction was a typical living polymerization. The peak at 7.92 ppm in the ^{1}H NMR spectrum (Figure 2) indicated the presence of a triazole ring, showing the success of the "click" coupling. Thus,

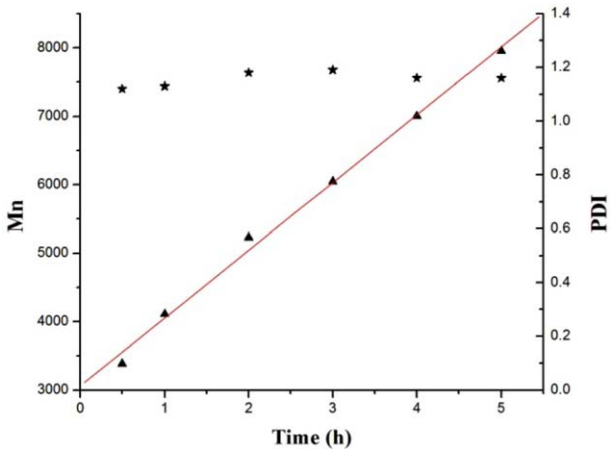

Figure 1. Typical first-order kinetic plot of furan-protected maleimido-terminated PEG_{600}-*b*-PSA. Reaction conditions: [Cu(I)Br]/[ligand]/[initiator]$_0$/[monomer]$_0$ = 1:5:1:40; T = 80°C. [Color figure can be viewed in the online issue, which is available at wileyonlinelibrary.com.]

the furan-protected maleimido-terminated PEG_{600}-*b*-PSA copolymer was obtained successfully in this one-pot method that combined a "click" reaction and ATRP. The polymer had a M_n (^{1}H NMR) of 7.6 × 10^3 and a M_w/M_n (GPC) equal to 1.19, which were calculated by comparison of the integrals of the triazole ring and the doublet of the acetal protecting group at 1.44 and 1.26 ppm.

The furan-protected maleimido-terminated PEG_{600}-*b*-PSA was first heated to 120°C to deprotect the furan group, leading to the disappearance of the peak corresponding to the double bonds in furan (δ = 6.51 ppm) and the appearance of the peak corresponding to the maleimido group (δ = 6.69 ppm) in the ^{1}H NMR spectrum [(Figure 3(A)]. Then, the deprotection of the ketal group was performed under acidic conditions until the solution turned transparent, signifying that the reaction had completed. The peak corresponding to the methyl group in the ketal (δ = 1.26 ppm) of the copolymer *N*-maleimido-terminated PEG_{600}-*b*-PGA had disappeared in the ^{1}H NMR spectrum [(Figure 3(B)]. All the conversions were almost complete, based on the ^{1}H NMR spectra.

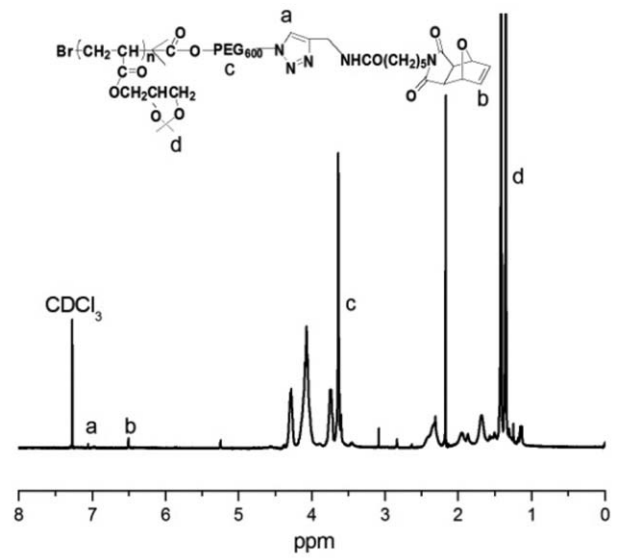

Figure 2. ^{1}H NMR spectrum of furan-protected maleimido-terminated PEG_{600}-*b*-PSA in $CDCl_3$.

FA has a γ-carboxyl group and an α-carboxyl group. When FA is covalently linked to a molecule via its γ-carboxyl moiety, its FR binding affinity ($K_d \sim 10^{-10} M$) remains essentially unaltered compared with free FA, and receptor-mediated endocytosis proceeds unhindered.[35,36] Fortunately, the γ-carboxyl of FA has higher reactivity than its α-carboxyl because of steric hindrance,[37] and the FA$^{\gamma}$ derivative is achieved in most reports.[14] In this work, Lys was attached to FA to enhance the solubility of FA derivatives in water. However, the coupling reaction between FA and the α-amino group of Lys hardly reacted because of steric hindrance. Therefore, Lys(FA)-Cys-NH_2 was synthesized, in which Cys offered the thiol group to enhance the reaction between Lys(FA)-Cys-NH_2 and *N*-maleimido-terminated PEG_{600}-*b*-PGA. The reaction was monitored by RP-HPLC as shown in Figure 4. The black line represented the initial mixture of *N*-maleimido-terminated PEG_{600}-*b*-PGA and Lys(FA)-Cys-NH_2, and the red line depicted the spectrum after the reaction had proceeded for 12 h. The peak height of Lys(FA)-Cys-

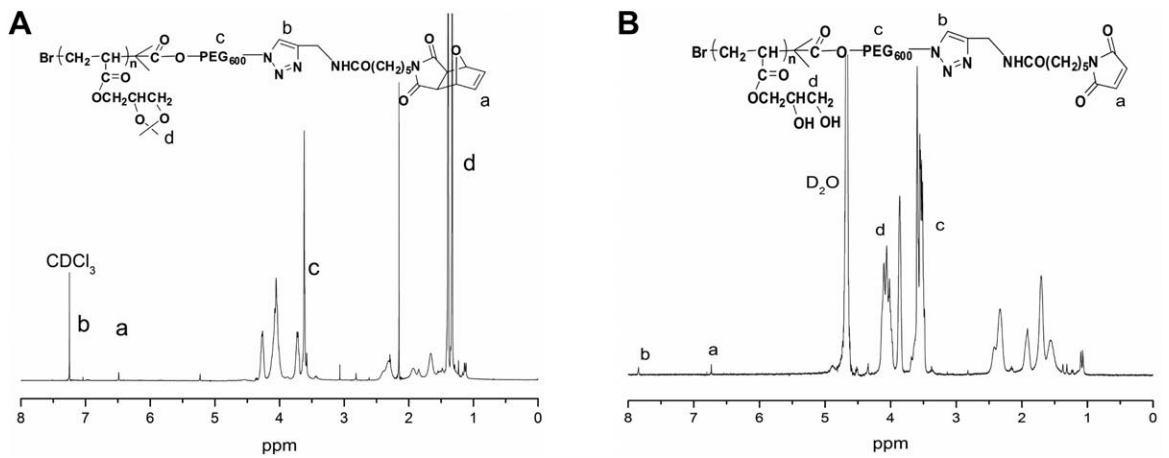

Figure 3. ^{1}H NMR spectrum of *N*-maleimido-terminated PEG_{600}-*b*-PSA (A) in $CDCl_3$ and *N*-maleimido-terminated PEG_{600}-*b*-PGA (B) in D_2O.

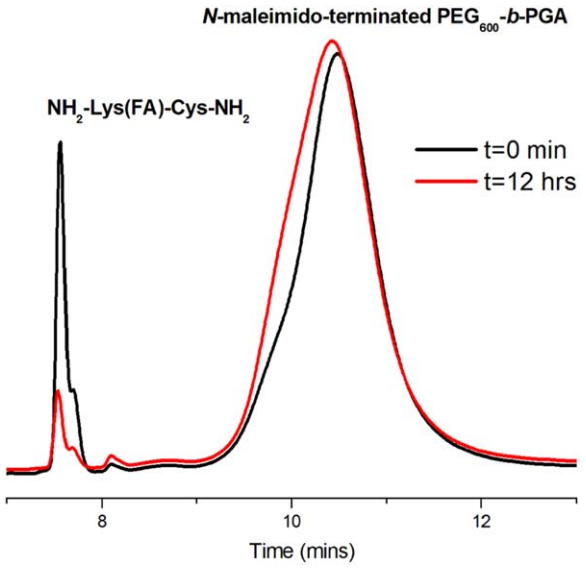

Figure 4. HPLC chromatogram of *N*-maleimido-terminated PEG_{600}-*b*-PGA+ Lys(FA)-Cys-NH_2. [Color figure can be viewed in the online issue, which is available at wileyonlinelibrary.com.]

NH_2 decreased upon reaction, and the resulting FA-PEG_{600}-*b*-PGA peak was clearly shifted to the left (high polarity). After dialyzation to remove the excess Lys(FA)-Cys-NH_2, the resulting polymer was analyzed to determine the purity using ^{1}H NMR (Figure 5). The peaks corresponding to the hydrogens of folate (a, b, c) appeared, and the maleimido group peak (6.69 ppm) disappeared, indicating that *N*-maleimido-terminated PEG_{600}-*b*-PGA was completely consumed. Compared with our previous work, FA-PEG_{600}-*b*-PGA was obtained in greater purity (95% purity, determined by UV absorption) with fewer reaction steps.

Characterization of FA-MNPs and FA-FITC-MNPs

FA-MNPs were obtained by FA-PEG_{600}-*b*-PGA complexation with the surface of $HClO_4$-stabilized Fe_3O_4 nanoparticles. FA-FITC-MNPs and mPEG-MNPs were prepared in the same manner. Figure 6 showed typical UV-visible absorption spectra of

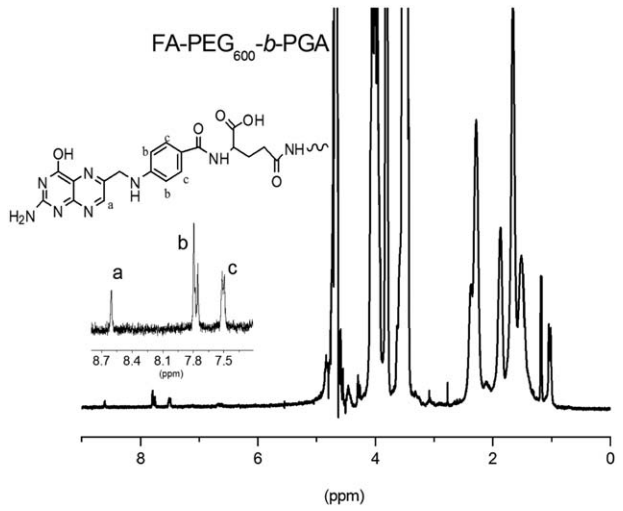

Figure 5. ^{1}H NMR spectrum of FA-PEG_{600}-*b*-PGA in D_2O.

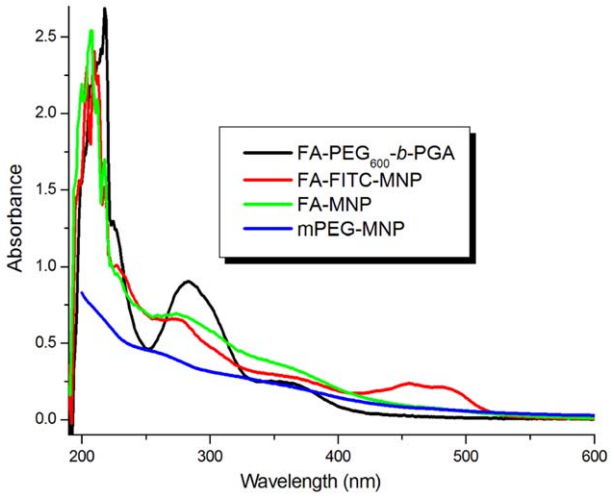

Figure 6. UV-visible absorption spectra of FA-conjugated polymer and magnetic nanoparticles. [Color figure can be viewed in the online issue, which is available at wileyonlinelibrary.com.]

FA-PEG_{600}-*b*-PGA (black line), FA-FITC-MNPs (red line), FA-MNPs (green line), and mPEG-MNPs (blue line). The characteristic absorption bands at approximately 280 nm from FA were all present in the three samples except mPEG-MNPs, demonstrating that FA-PEG_{600}-*b*-PGA was successfully incorporated into both FA-MNPs and FA-FITC-MNPs. The peak at 497 nm due to the FITC group was observed in FA-FITC-MNPs, also indicating that FITC-PEG_{600}-*b*-PGA was complexed with the MNPs.

The size distributions and ζ-potentials of the FA-MNPs and FA-FITC-MNPs were characterized using dynamic light scattering. As shown in Table I, the mean diameters of FA-MNPs and FA-FITC-MNPs were 77.83 ± 0.81 and 72.48 ± 1.13 nm, respectively, which were almost the same as those of the FITC-Tat-MNPs because of the same molecular weight of PEG_{600}-*b*-PGA.[33] The ζ-potential of FA-MNPs was -3.91 ± 0.36 mV; in contrast, that of FA-FITC-MNPs was -13.1 ± 1.03 mV, which was the sum of the anionic potentials of FITC-PEG_{600}-*b*-PGA and FA-PEG_{600}-*b*-PGA.

The aqueous dispersion of these nanoparticles could be stored at 4°C for months without significant precipitation, indicating that the aqueous dispersion of FA-MNPs is highly stable. Both of the $HClO_4$-stabilized MNPs and FA-MNPs showed superparamagnetic behavior without magnetic hysteresis according to SQUID magnetization at 300 K (Figure 7).

Cellular Uptake of FA-Conjugated Magnetic Nanoparticles

It has been reported that high-affinity folate receptors are overexpressed in different human cancers, whereas they have a significantly low expression in normal cells.[38,39] Herein, we use

Table I. Nanoparticle Properties

Sample	Mean diameter (nm)	ζ-Potential (mV)
FA-MNP	77.83 ± 0.81	-3.91 ± 0.36
FA-FITC-MNP	72.48 ± 1.13	-13.1 ± 1.03

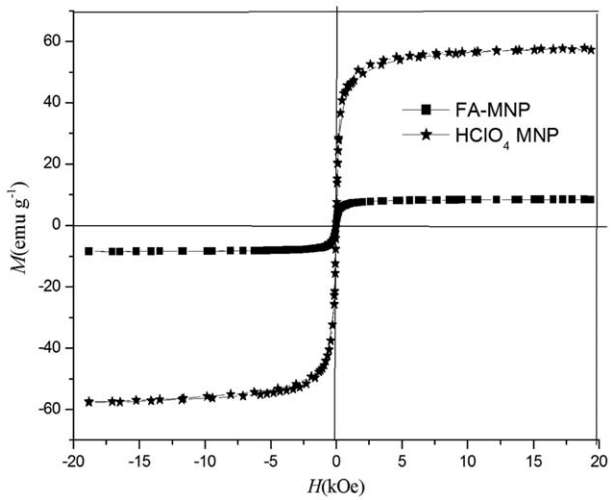

Figure 7. Room temperature magnetization curves of $HClO_4$ MNPs and FA-MNPs.

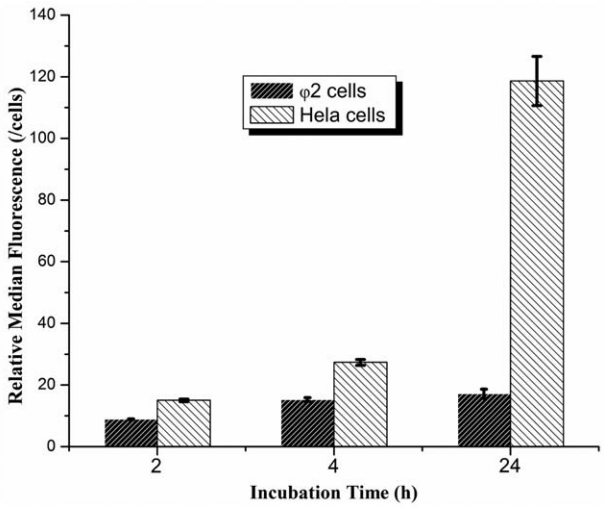

Figure 8. Intracellular uptake of FA-FITC-MNPs by Φ2 cells and Hela cells as a function of incubation time.

human cervical carcinoma Hela cells to investigate the specific targeting efficiency of folate-conjugated MNPs. $\varphi 2$ cells (normal cells) served as the control. It is well known that fluorescence techniques are popular methods to investigate the biological activity of nanocarriers.[40] Here, FITC was chosen as the fluorescence probe, and FA-FITC-MNPs were prepared. The cellular uptake of FA-FITC-MNPs in Hela cells and $\varphi 2$ cells, respectively, was monitored by FACS analysis. The RMF was obtained by dividing the median fluorescence of labeled cells by the median fluorescence of unlabeled cells, demonstrating the cellular uptake ability. After incubation with FA-FITC-MNPs for 24 h, the RMF intensity in Hela cells was five times greater than that in $\varphi 2$ cells. Thus, FA conjugation enhanced the internalization of nanoparticles by Hela cells via receptor-mediated endocytosis compared with $\varphi 2$ cells (Figure 8).

Live-cell imaging is a powerful tool to study particle internalization and to visualize particle localization in single cells. The cells were incubated in the FA-FITC-MNP solution for 60 min and then examined with live-cell imaging after washing with PBS to eliminate the disturbance of the nanoparticles solution. In Hela cells, a green color was obviously seen at the beginning, which almost coincided with the red color of the cell membrane stained with WGA, suggesting that the FA-FITC-MNPs were captured by the FRs on the surface of Hela cells (Supporting Information Video S1). As time went on, the green color gradually turned brighter, indicating that the FA-FITC-MNPs were internalized by the Hela cells. However, the green color remained nearly constant in the $\varphi 2$ cell membrane, even after recording for 60 min (Supporting Information Video S2). The fluorescence intensity density within a single cell was calculated to demonstrate the number of MNPs internalized. The fluorescence intensity density of the three Hela cells in Supporting Information Video S1 all increased as time progressed. However, it remained constant in the two $\varphi 2$ cells from Supporting Information Video S2 (Figure 9). These phenomena also confirmed that FA-FITC-MNPs could specifically target cancer cells. To determine whether FITC contributed to uptake by Hela cells or not, FITC-MNPs were incubated with Hela cells and $\varphi 2$ cells.

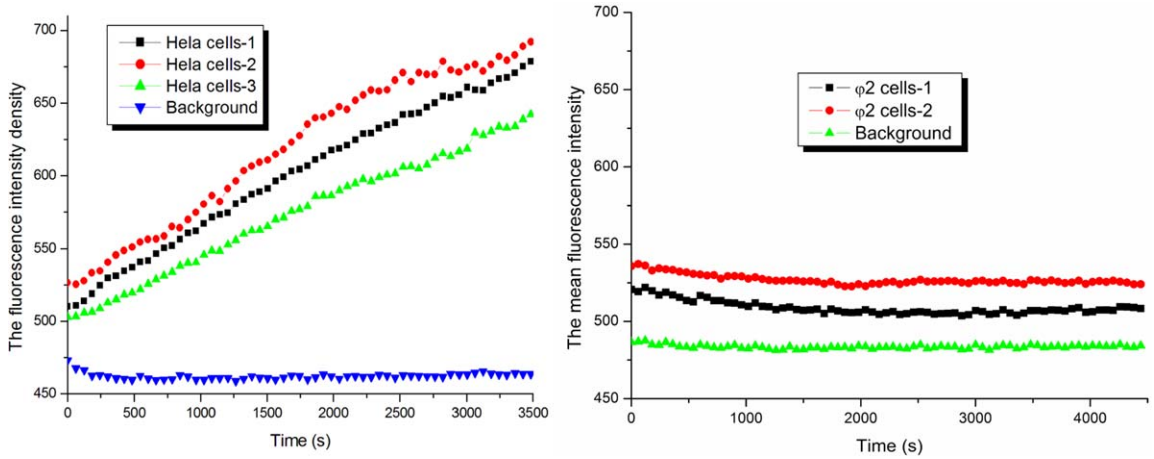

Figure 9. Change of fluorescence intensity density within the cells. [Color figure can be viewed in the online issue, which is available at wileyonlinelibrary.com.]

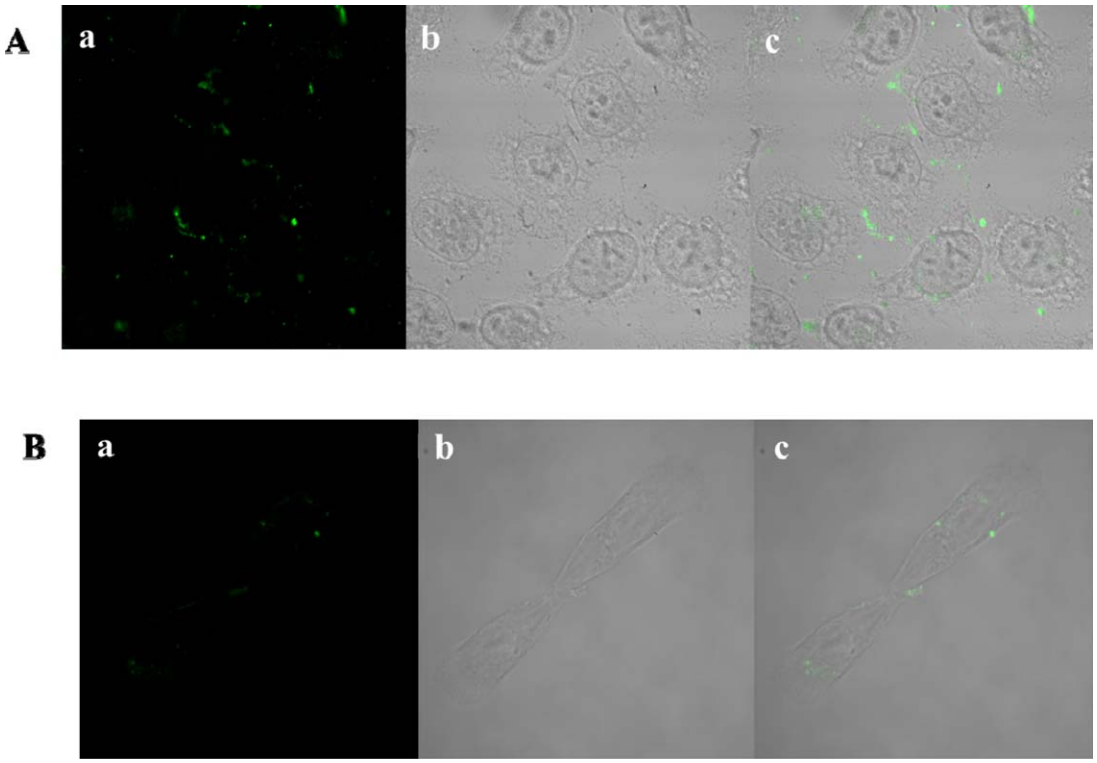

Figure 10. Confocal microscopy images showing FITC-MNPs incubated in Hela cells (A) and φ2 cells (B) for 2 h. (a) FITC-MNPs; (b) bright field; (c) merge of (a) and (b). [Color figure can be viewed in the online issue, which is available at wileyonlinelibrary.com.]

From confocal microscopy images shown in Figure 10, the green color of FITC-MNPs was scattered outside the cell membrane in both cases, indicating that FITC-MNPs could not uptake two kinds of cells. Thus, FA-FITC-MNPs exhibited the specially target ability only attribution to FA.

To further confirm that the FA-MNPs as a whole entered Hela cells, but not only the polymer FA-PEG_{600}-*b*-PGA alone, and to visualize the location of the nanoparticles inside the cells after internalization, TEM images of Hela cells cultured with FA-MNPs were obtained. For comparison, the cellular uptake of mPEG-MNPs was also investigated. Figure 11(A) shows the images of Hela cells treated with FA-MNPs. A higher magnification image [the inset of Figure 11(A)] reveals that dark dots of approximately 10–15 nm were found in the cell lysosomes. These dark dots should be the Fe_3O_4 nanocrystal images. However, nothing was found within the cells that were incubated with mPEG-MNPs, as shown in Figure 11(B). Thus, the folate-conjugates actually enhanced the tumor targeting of the magnetic nanoparticles and entered the Hela cells.

The nanoparticle toxicity index was obtained to determine whether the nanoparticles could be used *in vivo* or not. The cell viabilities of φ2 cells and Hela cells incubated with FA-MNPs

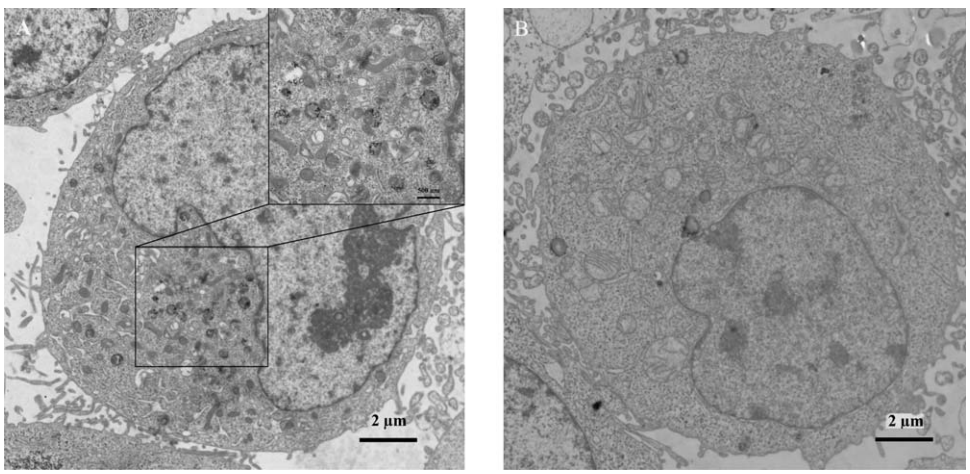

Figure 11. TEM images of FA-MNPs (A) and mPEG-MNPs (B) incubated with Hela cells for 24 h.

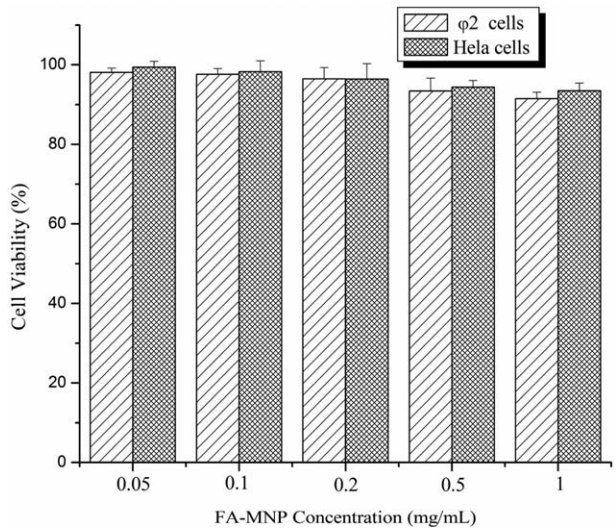

Figure 12. Cell viability of $\varphi 2$ cells and Hela cells treated with various concentrations of FA-MNPs as determined by the MTS assay. Results are means ± SD ($n = 5$).

were determined by the MTS assay. After 24 h of incubation, the viabilities of both types of cells were >90% even when the FA-MNP concentration was 1.0 mg/mL (Figure 12). No significant differences in cytotoxicity were observed between the two cell lines, although the extents of their cellular uptakes were different. These results indicated that FA-MNPs have low or no cytotoxicity toward these two types of cells and can be considered potentially safe for MRI or other *in vivo* applications.

CONCLUSION

After optimization of the synthetic procedure, the well-defined furan-protected maleimido-terminated PEG_{600}-*b*-PSA block copolymers were successfully synthesized in "one-pot" by the combination of a "click" reaction and ATRP using CuBr/PMDETA as the sole catalyst. The *N*-maleimido-terminated PEG_{600}-*b*-PGA block copolymer with high purity and yield was obtained after deprotection of the protecting groups. The copolymer could efficiently couple thiol groups on different compounds such as Lys(FA)-Cys-NH_2 and FITC-(ω-Ahex)-Cys-NH_2. Then, FA-MNPs with both FA donor and magnetic targeting functions for cancer cells were successfully prepared by assembly of FA-PEG_{600}-*b*-PGA with SPIONs. The uptake of FA-FITC-MNPs by Hela cells was approximately five times greater than that by normal $\varphi 2$ cells after incubation for 24 h and examined by FACS. Live-cell imaging showed the FA-FITC-MNPs could target and enter into Hela cells specifically. In addition, little black dots of Fe_3O_4 were found within the lysosome after culturing with FA-MNPs. In contrast, mPEG-MNPs were not found within the cell membrane of Hela cells as determined by TEM. Thus, FA-MNPs exhibited good biocompatibility with both cell lines.

ACKNOWLEDGMENTS

This work was supported by The National Key Technologies R & D Program for New Drugs of China (2012ZX09301003) and National Natural Science Foundation of China (81001417, 51373080).

REFERENCES

1. Torchilin, V. P. Nanoparticulates as drug carriers; Imperial College Press: London, **2006**, pp 397–411.
2. Ke, J. H.; Lin, J. J.; Carey, J. R.; Chen, J. S.; Chen, C. Y.; Wang, L. F. *Biomaterials* **2010**, *31*, 1707.
3. Yang, X. Q.; Pilla, S.; Grailer, J. J.; Steeber, D. A.; Gong, S. Q.; Chen, Y. H.; Chen, G. H. *J. Mater. Chem.* **2009**, *19*, 5812.
4. Yang, X. Q.; Grailer, J. J.; Rowland, I. J.; Javadi, A.; Hurley, S. A.; Steeber, D. A.; Gong, S. Q. *Biomaterials* **2010**, *31*, 9065.
5. Yang, X. Q.; Hong, H.; Grailer, J. J.; Rowland, I. J.; Javadi, A.; Hurley, S. A.; Xiao, Y. L.; Yang, Y. A.; Zhang, Y.; Nickles, R.; Cai, W. B.; Steeber, D. A.; Gong, S. Q. *Biomaterials* **2011**, *32*, 4151.
6. Toma, A.; Otsuji, E.; Kuriu, Y.; Okamot, K.; Ichikawa, D.; Hagiwara, A.; Ito, H.; Nishimura, T.; Yamagishi, H. *Br. J. Cancer* **2005**, *93*, 131.
7. Huang, G.; Zhang, C. F.; Li, S. Z.; Khemtong, C.; Yang, S. G.; Tian, R. H.; Minna, J. D.; Brown, K. C.; Gao, J. M. *J. Mater. Chem.* **2009**, *19*, 6367.
8. Kamat, M.; El-Boubbou, K.; Zhu, D. C.; Lansdell, T.; Lu, X. W.; Li, W.; Huang, X. F. *Bioconjugate Chem.* **2010**, *2*, 2128.
9. Nasongkla, N.; Bey, E.; Ren, J. M.; Ai, H.; Khemtong, C.; Guthi, J. S.; Chin, S. F.; Sherry, A. D.; Boothman, D. A.; Gao, J. M. *Nano Lett.* **2006**, *6*, 2427.
10. Lu, Y.; Low, P. S. *Adv. Drug Deliv. Rev.* **2002**, *54*, 675.
11. Ross, J. F.; Chaudhuri, P. K.; Ratnam, M. *Cancer* **1994**, *73*, 2432.
12. Sudimack, J.; Lee, R. J. *Adv. Drug Deliv. Rev.* **2000**, *41*, 147.
13. Sonvico, F.; Mornet, S.; Vasseur, S.; Dubernet, C.; Jaillard, D.; Degrouard, J.; Hoebeke, J.; Duguet, E.; Colombo, P.; Couvreur, P. *Bioconjugate Chem.* **2005**, *16*,1181.
14. Sun, C.; Sze, R.; Zhang, M. Q. *J. Biomed. Mater. Res.* **2006**, *78A*, 550.
15. Chao, H.; Koon-Gee, N.; En-Tang, K. *Langmuir* **2012**, *28*, 563.
16. Wan, S. R.; Zheng, Y.; Liu, Y. Q.; Yan, H. S.; Liu, K. L. *J. Mater. Chem.* **2005**, *15*, 3424.
17. Zhang, Q.; Wang, C. H.; Qiao, L.; Yan, H. S.; Liu, K. L. *J. Mater. Chem.* **2009**, *19*, 8393.
18. Kolb, H. C.; Finn, M. G.; Sharpless, K. B. *Angew. Chem. Int. Ed.* **2001**, *40*, 2004.
19. Tornoe, C. W.; Christensen, C.; Meldal, M. *J. Org. Chem.* **2002**; *67*, 3057.
20. Rostovtsev, V. V.; Green, L. G.; Fokin, V. V.; Sharpless, K. B. *Angew. Chem. Int. Ed.* **2002**, *41*, 2596.
21. Wang, J. S.; Matyjaszewski, K. *J. Am. Chem. Soc.* **1995**, *117*, 5614.
22. Matyjaszewski, K.; Xia, J. H. *Chem. Rev.* **2001**, *101*, 2921.
23. Kamigaito, M.; Ando, T.; Sawamoto, M. *Chem. Rev.* **2001**, *101*, 3689.
24. Coessens, V.; Pintauer, T.; Matyjaszewski, K. *Prog. Polym. Sci.* **2001**, *26*, 337.

25. Topham, P. D.; Sandon, N.; Read, E. S.; Madsen, J.; Ryan, A. J.; Armes, S. P. *Macromolecules* **2008**, *41*, 9542.
26. Xu, L. Q.; Yao, F.; Fu, G. D.; Shen, L. *Macromolecules* **2009**, *42*, 6385.
27. Li, Q. X.; Dong, W.; Huifen, F. G.; Koon-Gee, N.; En-Tang, K.; Guo, D. F. *Langmuir* **2010**, *26*, 15376.
28. Chen, X. J.; McRae, S.; Parelkar, S.; Emrick, T. *Bioconjugate Chem.* **2009**, *20*, 2331.
29. Pan, C.; Tao, L.; Wu, D. *J. Polym. Sci. Part A: Polym. Chem.* **2001**, *39*, 3062.
30. Wang, C. H.; Qiao, L.; Zhang, Q.; Yan, H. S.; Liu, K. L. *Int. J. Pharm.* **2012**, *430*, 372.
31. Mantovani, G.; Lecolley, F.; Tao, L.; Haddleton, D. M.; Clerx, J.; Cornelissen, J. J. L. M.; Velonia, K. *J. Am. Chem. Soc.* **2005**, *127*, 2966.
32. Parrish, B.; Breitenkamp, R. B.; Emrick, T. *J. Am. Chem. Soc.* **2005**, *127*, 7404.
33. Deng, G.; Chen, Y. *Macromolecules* **2004**, *37*, 18.
34. Liu, S.; Elyashiv, S.; Sen, A. *J. Am. Chem. Soc.* **2001**, *123*, 12738.
35. Reddy, J. A.; Low, P. S. *Crit. Rev. Ther. Drug Carrier Syst.* **1998**, *15*, 587.
36. Ke, C. Y.; Mathias, C. J.; Green, M. A. *Adv. Drug Deliver. Rev.* **2004**, *56*, 1143.
37. Gabizon, A.; Horowitz, T.; Goren, D.; Tzemach, D.; Mandelbaum-Shavit, F.; Qazen, M. M.; Zalipsky, S. *Bioconjugate Chem.* **1999**, *10*, 289.
38. Zheng, X.; Kelley, K.; Elnakat, H.; Yan, W.; Dorn, T.; Ratnam, M. *Mol. Cell Biol.* **2003**, *23*, 2202.
39. Antony, A. *Adv. Drug. Deliver. Rev.* **2004**, *56*, 1059.
40. Kasten, F. H. In Fluorescent and Luminescent Probes for Biological Activity; Introduction to Fluorescent Probes: Properties, History, and Applications in, W.T. Mason, Ed., Academic Press: New York, **1993**, pp 12–33.